A perspective on creep and fatigue issues in sodium cooled fast reactors

Article *in* Transactions of the Indian Institute of Metals · April 2010

DOI: 10.1007/s12666-010-0011-3

CITATIONS
25

READS
1,081

2 authors:

Baldev Raj
Indira Gandhi Centre for Atomic Research
919 PUBLICATIONS **18,386** CITATIONS
SEE PROFILE

B.K. Choudhary
Indira Gandhi Centre for Atomic Research, Kalpakkam - 603102, India
165 PUBLICATIONS **2,211** CITATIONS
SEE PROFILE

Transactions of The Indian Institute of Metals
Vol. 63, Issues 2-3, April-June 2010, pp. 75-84

A perspective on creep and fatigue issues in sodium cooled fast reactors

Baldev Raj and B.K. Choudhary

Indira Gandhi Centre for Atomic Research, Kalpakkam - 603 102, Tamil Nadu, India

E-mail : bkc@igcar.gov.in

Received 1 June 2010
Revised 10 June 2010
Accepted 10 June 2010
Online at www.springerlink.com

Keywords:
Creep; fatigue; austenitic stainless steel; ferritic steel

Abstract

Development of advanced materials alongwith improved high temperature mechanical properties, particularly creep and fatigue are important and play a major role for the successful development of robust, safe and economical sodium cooled fast reactor (SFR) technology. The components of SFRs operate in demanding environments at high temperatures under complex creep, fatigue and creep-fatigue loading conditions. Based upon the service requirements in terms of different environments, temperature and loading conditions, different materials are chosen for different components. Ti modified 15Cr-15Ni austenitic stainless steel is chosen for clad and wrapper tubes in the reactor core, which experience high fast neutron flux of ~ 10^{15} $ncm^{-2}s^{-1}$ along with high temperatures. Type 316L(N) SS is used for out-of-core structural components like main and inner vessels, and sodium pipelines. For steam generators, modified 9Cr-1Mo steel is chosen for all the components, where liquid sodium and steam/water coexist. Some of the important experiences and exciting achievements in the areas of in-house materials development and its characterization in terms of creep, low cycle fatigue and creep-fatigue properties important to design of reactor components for core, out-of-core and steam generator applications are described in the paper. Future directions for materials research and development activities involving critical issues like radiation damage resistance along with improved mechanical properties for advanced clad and wrapper materials necessary for achieving high fuel burnup and design life up to 60 years for out-of-core structural components leading to economical nuclear energy have been highlighted.

1. Introduction

Indices of socio-economic development like literacy, longevity, gross domestic product (GDP) and development in human resources are directly related to per capita energy consumption. The energy and electricity growths are closely linked to growth in economy. India is aiming to reach per capita energy consumption at least equal to the present world average of 2200 kWh/a by 2030 from the current value of 660 kWh/a. The current installed capacity of ~ 143 GWe (as on March 2008), needs to be increased to about 600 GWe by 2030 assuming the increased population of ~ 1.4 billion. Energy strategists in the country have realised the importance of judicious mix of energy resources to meet this challenge. A large share of nuclear energy is an inevitable choice from resources, sustainability and environmental considerations. The nuclear energy is expected to contribute about 63 GWe by 2030, which will be steadily increased to 275 GWe by 2052, against the total projected capacity of 1344 GWe. This would be realized through water reactors in the 1st stage, sodium cooled fast breeder reactors (SFRs) with high breeding in the 2nd stage and thorium based reactors in the 3rd stage [1]. India has limited resource of natural uranium, but has vast resource of thorium. In order to have the best utilization of theses resources, the development of fast breeder reactors with closed fuel cycle is inevitable for the country.

India started its FBR programme by constructing a sodium cooled loop type 40 MWt (13.2 MWe) experimental Fast Breeder Test Reactor (FBTR) at Kalpakkam. FBTR was commissioned in 1985 with a unique plutonium rich carbide fuel. First of its kind plutonium-uranium carbide fuel in FBTR has achieved a burnup of 163 GWd/t without any clad failure. Based on the gain from the world over operating experiences of ~ 390 reactor years including FBTR, and comprehensive science based research and technology development programme, the design and technology of 500 MWe Prototype Fast Breeder Reactor (PFBR) with mixed oxide (MOX) fuel has been established [1]. Presently, the PFBR is under construction and is scheduled for commissioning in 2011. PFBR is a pool type reactor with 2 primary and 2 secondary loops with 4 steam generators per loop. The design life is 40 years with at least 75% load factor to be successively enhanced to 85%. The main vessel houses the hot and cold sodium pools, which are separated by inner vessel. The reactor core, consisting of large number of subassemblies including fuel subassemblies, is supported on a grid plate. The nuclear heat generated in the core is removed by circulating sodium from cold pool at 670 K to the hot pool at 820 K to four intermediate heat exchangers (IHX). The heat from IHX is transported to eight steam generators (SG) by sodium flowing in the secondary circuit. Steam produced in SG is supplied to turbo-generator.

The science and engineering of SFRs is muliti-faceted and multi-directional in nature and spread over physics/ neutronics to waste management involving several important and key issues in different areas in-between. Further, the development of robust, safe and economical SFR technology throws numerous challenges in various domains such as the development of advanced materials, innovative design

optimisation and reliable structural mechanics analysis, sound manufacturing technology, testing and evaluation of critical components, mature pre-service and in-service non-destructive evaluation, and post-irradiation examination techniques [1]. Among the research areas being pursued to realise the ambitious goal on SFR programme in the country, research on materials remains on the top of the list for achieving high fuel burnup, long design life and high temperatures. Based on the service and operating environments, materials are grouped as for core, out-of-core and steam generator applications in SFRs [1,2]. The components of reactor core, out-of-core and steam generators experience high temperatures with varying gradients, different modes of loading such as creep, fatigue and creep-fatigue and different environments. For example, the core materials are subjected to a very demanding environment of high fast neutron flux (~10^{15} $ncm^{-2}s^{-1}$) coupled with high temperatures. The major phenomena that have impact on the performance of core components include phase stability, void swelling, irradiation creep including thermal creep and associated changes in mechanical properties. Void swelling, irradiation creep and irradiation embrittlement are important to both clad (housing fuel pins) and wrapper (housing several clads) that determine the residence time of fuel elements in the core and effective fuel burnup for nuclear energy economy. Non-uniform deformations and differential void swelling occurring due to gradients in neutron flux and temperature at different locations in the core can lead to several operational problems and affect the reactivity of the core. Materials for core components have evolved continuously over the years resulting in substantial improvement in the fuel element performance. The first generation materials belonged to 304 and 316 SS grades. These steels quickly reach their limits because of unacceptable swelling at doses higher than ~ 50 dpa. Many improvements were made by the addition of stabilising elements, changes in the major and minor elements addition and modifications of the microstructure such as cold working. This has led to the development of new core material such as 15Cr-15Ni-2.5Mo-Ti steel, Alloy D9 with reduced Cr, increased Ni content and controlled Ti addition in 316 SS and its variants D9I (with increased Si and P) for which the incubation dose for swelling is quite high [3-5]. Further, for doses above 120 dpa, austenitic stainless steels are difficult to be employed, as void swelling is found to be unacceptable. Ferritic/martensitic steels such as modified 9Cr-1Mo and Sandvik HT9, though exhibit high void swelling and irradiation creep resistance, have poor thermal creep strengths at temperatures above 823-873 K and this restricts the high burnup of fuel with clad operating in the temperature range 873-973 K [6-8]. Oxide dispersion strengthening (ODS) appears to be the promising means of extending creep resistance of ferritic/martensitic steels beyond 923 K without sacrificing the inherent advantages of high thermal conductivity and low swelling of ferritic steels [9,10].

For our-of-core applications, austenitic stainless steel 316 L(N) is the major structural material for main vessel, inner vessel and the hot pipelines of PFBR [1,2]. Selection of reduced carbon and controlled nitrogen added L(N) grades of austenitic stainless steels for out-of-core applications is driven mainly by significant reduction in sensitization resulting in high resistance to stress corrosion cracking and also improved high temperature mechanical properties over conventional grades. Modified 9Cr-1Mo (Grade 91) steel is selected for all the components (shell, tube and tube sheet) for steam generator applications following mono-metallic concept, where sodium and water co-exist. The selection of G91 steel is mainly based on its higher creep and low cycle fatigue resistance than those exhibited by its counterparts like plain 9Cr-1Mo and 2.25-1Mo steels. Further, use of G91 steel eliminates the problems of sensitization generally encountered in stainless steels.

A comprehensive materials research activity at IGCAR, Kalpakkam is directed towards the development and characterisation of materials for core, out-of-core structure and steam generator applications in SFRs [1]. Evaluation of mechanical properties such as tensile, creep, low cycle fatigue, creep-fatigue and fracture required for design purposes, strength-microstructure correlation, assessment of creep and fatigue damages, detailed analysis and reliable extrapolation of data, and modelling are important research activities pursued at this centre. Weld and weld joints are known to be the weak links and life limiting regions of a component. Welding science and technology research activities for austenitic and ferritic steels are aimed to obtain defect-free welds with optimum high temperature mechanical properties particularly creep and fatigue of the weld joints. Special emphasis has been placed to improve the generic hot cracking resistance in austenitic steels and type IV cracking resistance in ferritic steels. Detailed analysis of strain-time creep data in terms of unified approach and first order kinetics resulted in obtaining master creep curves (one interrelating transient creep and secondary creep and another interrelating tertiary creep and secondary creep) and new creep rate-time relationships of Monkman-Grant type [11,12]. Recently, a creep damage criterion has been introduced based on the seminal concept of time to reach Monkman-Grant ductility (the product of creep rate and rupture time) as the time where the secondary creep ductility is exhausted along the creep curve, the true tertiary creep sets in and damage attains a critical level [13]. The critical creep damage criterion was obtained using Continuum Damage Mechanics (CDM) approach, Material's Properties Council (MPC)-Omega approach and θ-Projection method, interrelating the time to reach Monkman-Grant ductility with rupture life that depends only on damage tolerance factor [14-16]. The validity has been demonstrated for a wide range of materials and its useful implications to tertiary creep and engineering creep design have been proposed. In the following, some of the recent results and outcome of the research activities dealing with creep, fatigue and creep-fatigue issues in materials for core, our-of-core and steam generators are briefly described. Future directions for the research and development of improved creep, fatigue and radiation damage resistant new and advanced materials for achieving high breeding ratio and high fuel burnup leading to economical nuclear energy have been highlighted.

2. Creep and fatigue behaviour of reactor and SG materials - recent results and important outcome

2.1 Core structural material - improvement in creep properties of alloy D9

The effect of Ti/C ratio on the creep rupture properties of Alloy D9 bulk material processed as rounds is shown in Fig. 1 at 973 K [17]. The highest rupture strength was exhibited by the heat containing Ti/C = 4 and the lowest rupture strength by the heat containing Ti/C = 6. Rupture ductility was generally lower than 10%, and the lowest ductility was obtained for the alloy having ratio of Ti/C = 4.

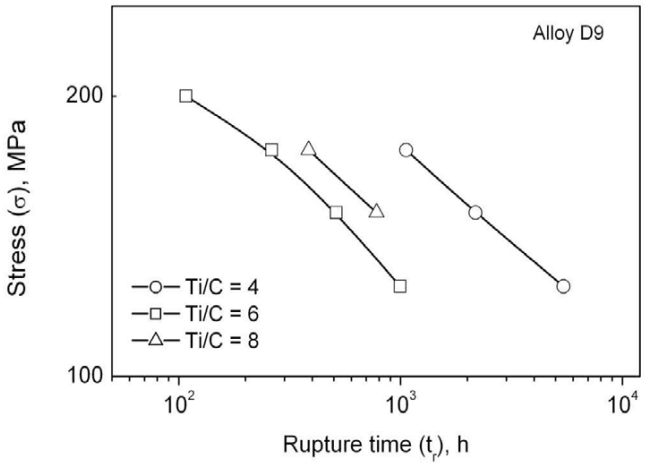

Fig. 1 : Influence of Ti/C on creep life of 20% cold worked Alloy D9 at 973 K [17].

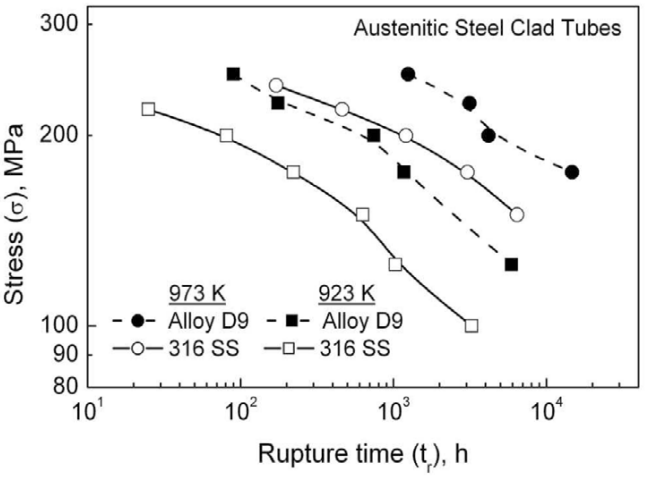

Fig. 2 : Comparison of creep-rupture strength Alloy D9 and type 316 SS clad tubes at 923 and 973 K [18].

The comparison of rupture lives of alloy D9 and 316 SS clad tubes at 923 and 973 K are shown in Fig. 2 [18]. Alloy D9 exhibited superior creep-rupture strength than that of 316 SS at 923 and 973 K. The improvement in strength of alloy D9 was found to be the consequence of prolonged secondary creep stage. The failure during creep of Alloy D9 was characterised typically by intergranular cracking as shown in Fig. 3.

Austenitic stainless steels derive their strength from solid solution strengthening as well as from carbide precipitation in the matrix. In the case of 316 SS, fine $M_{23}C_6$ carbides form at 873 K. At 973 K and above, coarsening of carbides results in recovery and thereby leads to the decreased efficiency of precipitation strengthening. In Alloy D9, carbon is partitioned between titanium and chromium. Chromium carbide forms preferentially along the grain boundaries, whereas fine secondary titanium carbides form predominantly in the matrix thereby imparting higher creep rupture strength. The higher creep strength of alloy D9 is derived from the fine and stable TiC precipitation during thermo-mechanical treatments. This also plays a crucial role in delaying the onset of void swelling as well as its high performance in reactor environment (Fig. 4a). The origin of this microstructural stability lies in part in the orientation relationship of the precipitates with austenite matrix [19]. The fine scale precipitation characteristics of titanium carbides in alloy D9 has been

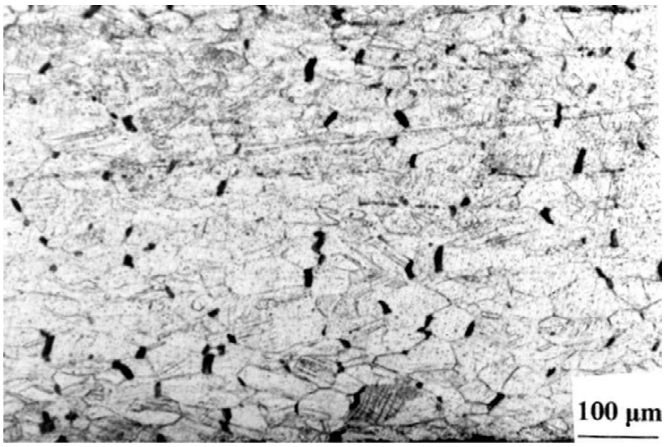

Fig. 3 : Alloy D9 showing intergranular cracking characterised by wedge cracks in specimen tested at 175 MPa at 923 K.

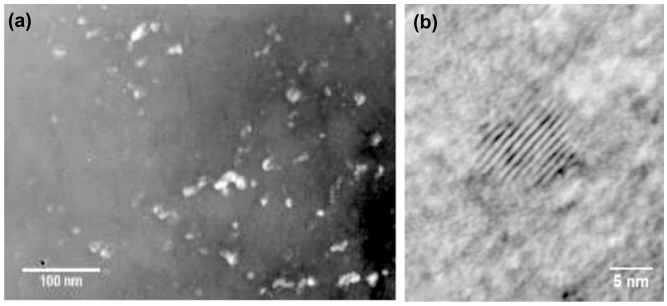

Fig. 4 : (a) Fine scale precipitation of TiC in alloy D9 aged at 550°C for 24 h. High magnification image with moiré fringes due to fine scale TiC is shown in (b).

investigated by lattice imaging techniques as shown in Fig. 4b. It has been also seen that the nanoscale titanium carbide precipitates in the cold worked samples show deviations to the extent of a few degrees from the ideal orientation relationship.

2.2 Out-of-core structural materials

2.2.1 Influence of nitrogen - improved creep-rupture properties of type 316L(N) SS and its weld

In order to minimise sensitisation and associated stress corrosion cracking problems in austenitic steels, the carbon has been reduced to 0.02-0.03% with addition of nitrogen in the range 0.06-0.08% along with close control of other alloying and minor elements in 316L(N) SS for PFBR applications. Nitrogen is added to compensate for the loss in solid-solution strengthening due to the reduced carbon content in the steel. Figure 5 shows a comparison of creep-rupture strength for 316L(N) and 316 stainless steels at 873 K [20,21]. Significant increase in creep-rupture strength was observed for the steel containing 0.07% nitrogen compared to that of 316 SS. The beneficial effects of nitrogen is accrued from higher solubility of nitrogen in the matrix than the carbon, reduction in stacking fault energy of the matrix and introduction of strong elastic distortions into the crystal lattice, giving rise to strong solid solution strengthening [22]. Nitrogen also effects the diffusivity of chromium in austenitic stainless steels leading to retardation in coarsening of $M_{23}C_6$ thereby retaining the beneficial effects of carbide precipitation for long durations [21,22].

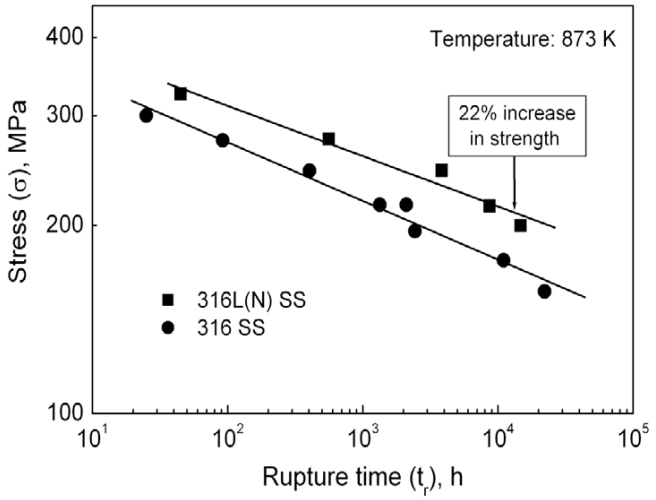

Fig. 5 : Stress vs. rupture time plots for type 316 and 316L(N) stainless steel at 873 K showing improved creep-rupture strength of 316L(N) SS [22].

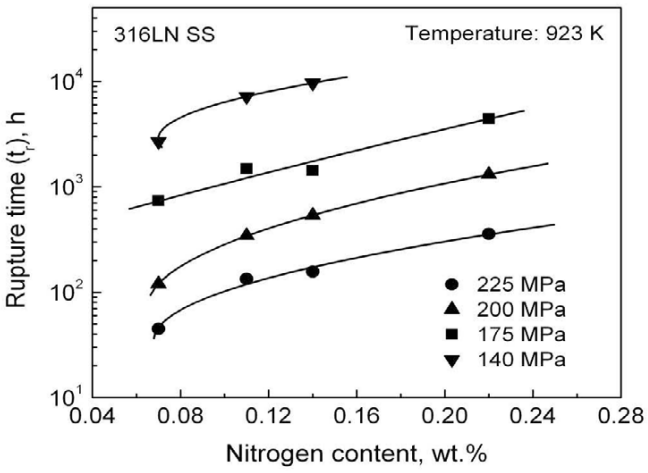

Fig. 6 : Influence of nitrogen on creep-rupture strength of 316LN SS at 923 K [23].

A systematic investigation on the influence of nitrogen on creep behaviour of 316LN stainless steel revealed that the creep-rupture strength increases substantially with increase in nitrogen content [23]. Figure 6 shows an example at 923 K. Rupture life increased by an order of magnitude with increase in nitrogen from 0.07 to 0.22%. The increase in creep strength with increase in nitrogen content was associated with decrease in steady state creep rate, and increase in time spent in primary as well as secondary creep stages leading to increase in time to onset of tertiary creep. A similar increase in time spent in tertiary creep with increasing nitrogen was also displayed. TEM investigations revealed rearrangement of dislocations into subgrains following creep exposure in steel having 0.07% nitrogen. The tendency to form subgrains decreases with increasing nitrogen content indicating reduced dynamic recovery in high nitrogen steels. Further, the grain boundary cracking on the surface and in the interior decreased substantially with increase in nitrogen content as shown in Fig. 7.

Detailed investigations on the creep behaviour of weld metal and weld joint at 823, 873 and 923 K has shown that weld metal exhibit the lowest creep-rupture strength compared to weld joint and base metal [22]. Figure 8 shows the comparison of creep strength of base metal, weld metal and weld joint at 873 K as an example. The creep strength of weld joint lies in between of those for base and weld metals. At all the three temperatures, the experimental data for the base metal, weld metal and weld joint lie well above the RCC-MR average curve for the weld joint.

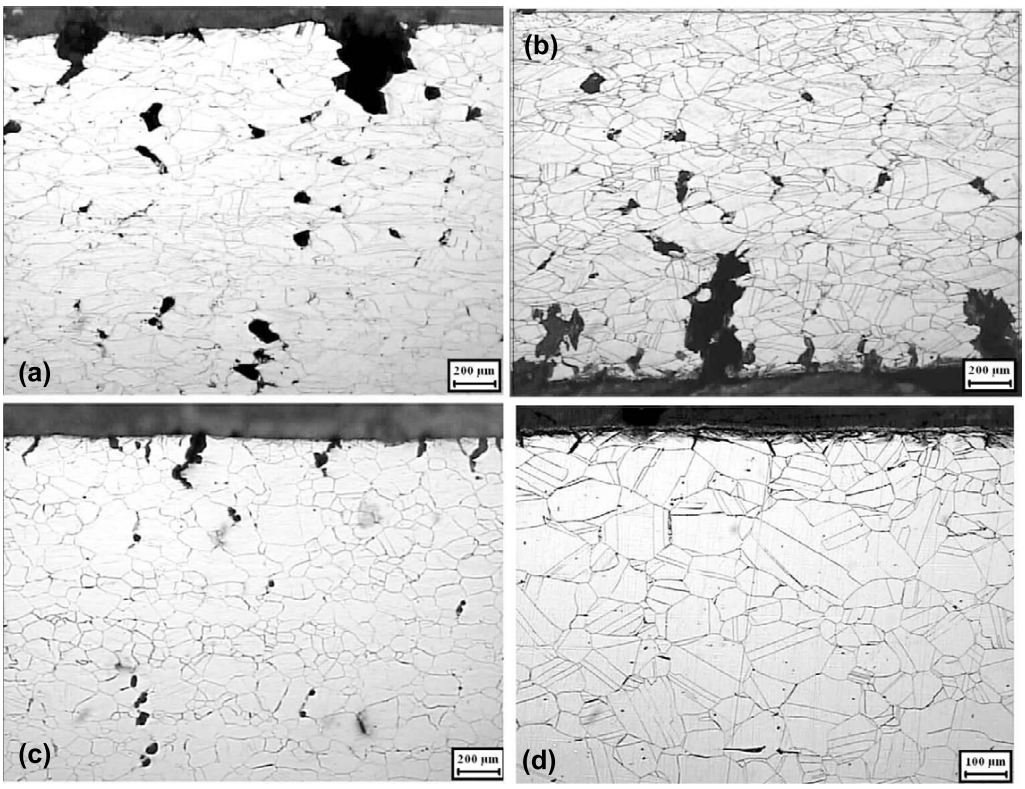

Fig. 7 : Influence of (a) 0.7 (b) 0.11 (c) 0.14 and (d) 0.22% nitrogen on intergranular cracking on the surface and interior at 923 K and at 225 MPa in 316LN steel [23].

2.2.2 *Low cycle fatigue properties of 316L(N) SS base, weld and weld joint*

Variations of fatigue life with strain rate at 773, 823 and 873 K are shown in Fig. 9 [24]. At all temperatures, fatigue life decreased with decrease in applied strain rate. Generally, a systematic decrease in life was seen with increase in temperature. However, a cross-over has been observed between 823 and 873 K at intermediate strain rates, where the LCF lives obtained at 873 K were higher than the lives at lower temperature of 823 K at low strain amplitudes. Decrease in fatigue life with decreasing strain rate at 773 and 873 K as well as at 873 K for high strain rate regime has been ascribed to the dominance of dynamic strain ageing (DSA) as manifested by serrated flow, significant cyclic hardening and negative strain rate sensitivity on flow stress as shown in Fig. 10 [24,25]. In the DSA dominated regime, the half-life stress value increases rapidly with decrease in strain rate (Fig. 10) and the fracture mode is dominated by mixed mode fracture. Contrary to this, dynamic recovery and oxidation effects in the low strain rate regime at 873 K resulted in decrease in flow stress and LCF life with decrease in strain rate. The two different regimes are distinguished by the dominance of planar slip in the DSA regime (Fig 11a) and the formation of dislocation cell structure in the creep regime (Fig. 11b). The cross-over in the LCF life observed for

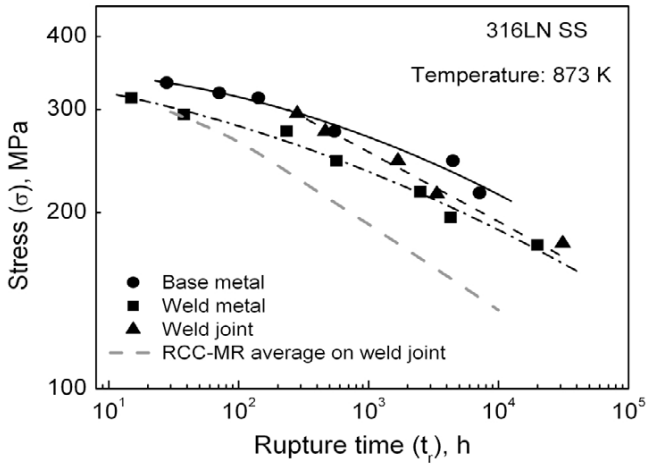

Fig. 8 : Comparison of the creep-rupture strength of base metal, weld metal and weld joint of 316L(N) stainless steel at 873 K [22].

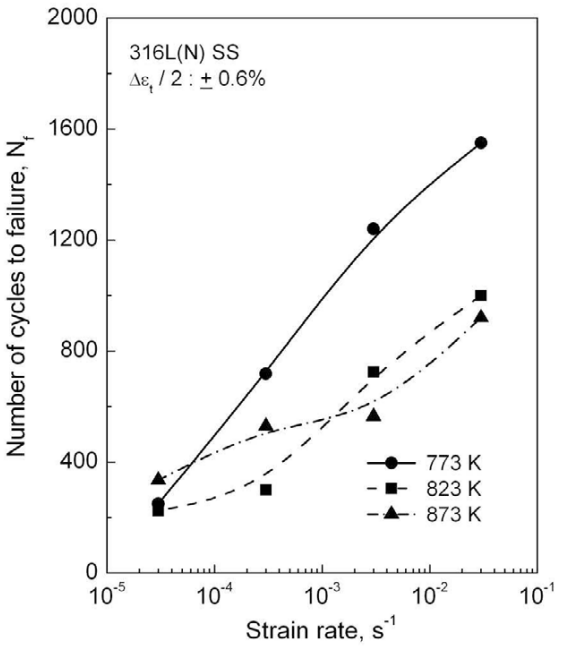

Fig. 9 : Variations of fatigue life of 316L(N) SS showing decrease in the life with decreasing strain rate at 773, 823 and 873 K [24].

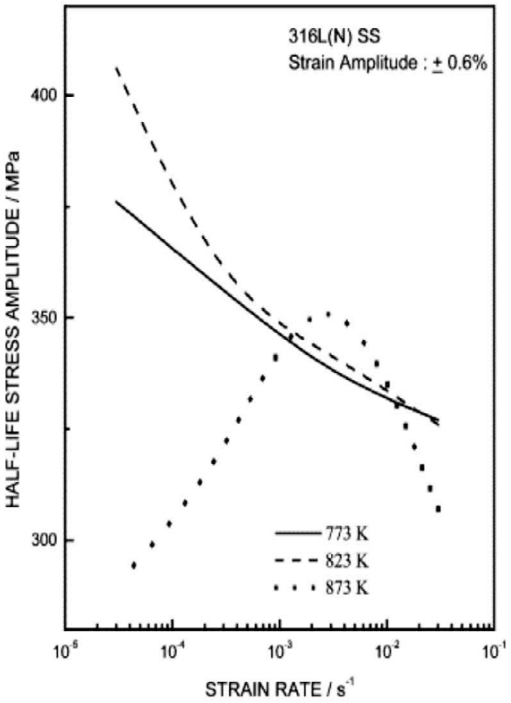

Fig. 10 : Variations of half-life stress with decreasing strain rate for 316L(N) SS at 773, 823 and 873 K. Increase in half-life stress with decrease in strain rate is due to dynamic strain ageing, while decrease in half-life stress at low strain amplitudes at 873 K is ascribed to creep effects [24].

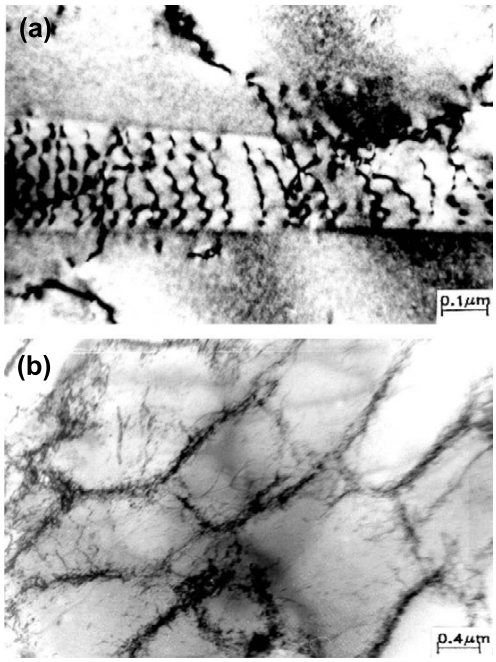

Fig. 11 : Typical TEM micrographs showing dominance of (a) planar slip in the DSA regime and (b) well defined dislocation cell structure in the creep regime [24].

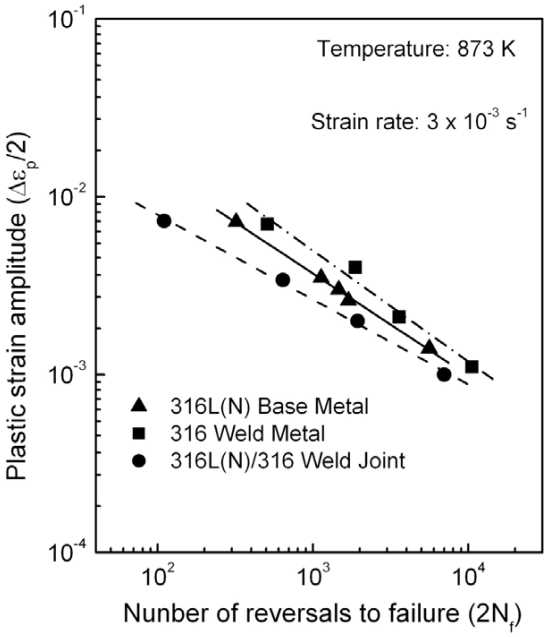

Fig. 12 : Plastic strain-life plots for 316L(N) base metal, weld metal and weld joint at 873 K.

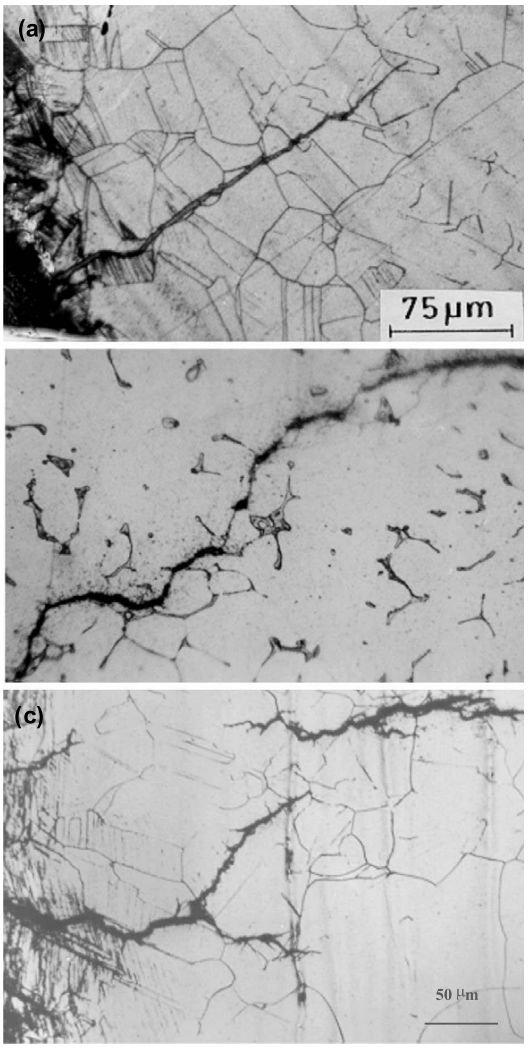

Fig. 13 : Optical micrographs showing (a) crack initiation and propagation in base metal (b) crack propagation in weld metal and (c) crack initiation and propagation in coarse grain HAZ of 316L(N) SS tested at 873 K.

873 K results from the influence of two or more competing processes e.g., domination of DSA effects in high strain rate regime and creep effects in low strain rate regime. Reduced contribution or absence of dominant DSA could have resulted in higher LCF life in the low strain rate regime at 873 K than at 823 K. A substantial decrease in fatigue life due to combined influence of creep and oxidation damages was observed with increase in tensile hold indicating creep-fatigue-environment interaction in 316L(N) SS [25].

Comparative evaluation of LCF resistance of base metal, weld metal and weld joints of 316L(N) SS indicated that weld joint display inferior fatigue life compared to that of base and weld metals. Figure 12 shows the above comparison at 873 K as an example. Weld metal exhibits higher fatigue life than the base metal. The inferior LCF resistance of weld joints is ascribed to shortening of crack initiation in coarse grain heat affected zone (HAZ) (Fig. 13c). The superior LCF resistance of weld metal (Fig. 13b) appears to result from the deflection of propagating cracks at transformed delta-ferrite.

2.2.3 Thermo-mechanical fatigue of 316L(N) SS

Thermomechanical fatigue (TMF) behaviour of 316L(N) stainless steel was examined under different temperature domains. Cylindrical hollow and smooth specimens were subjected to in-phase (IP) and out-of-phase (OP) thermal-mechanical cycling using mechanical strain control mode at a strain rate of 6.4×10^{-5} s^{-1} and a strain amplitude of ± 0.4% [26]. The TMF life was seen to decrease with increasing peak and mean temperatures of thermal cycling (Fig. 14). It was noticed that TMF life in out-of-phase cycling is lower than

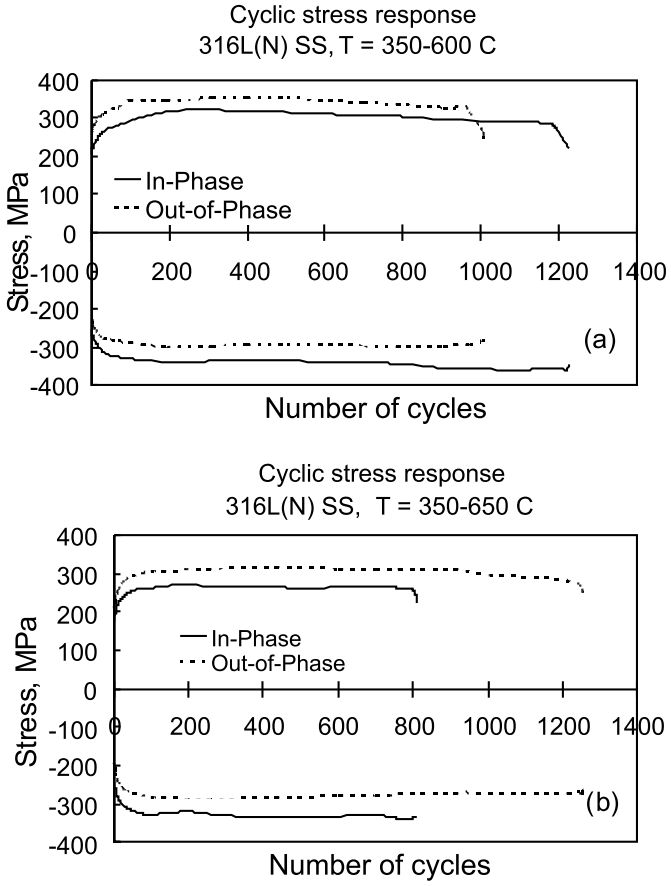

Fig. 14 : Comparative stress response between in-phase and out-of-phase thermo-mechanical fatigue in the temperature range (a) 623-873 K and (b) 623-923 K [26].

that in the in-phase tests when the maximum temperature of TMF cycling (T_{max}) was less than or equal to 873 K (Fig. 14a), while in the creep temperature domain (T_{max} = 923 K), the IP tests yielded lower lives, (Fig. 14b). The lower life of the alloy in the OP testing conditions in the lower temperature regimes could be attributed to the development of a tensile mean stress and the higher stress level leading to an early crack initiation and a faster propagation. However, under conditions wherein the T_{max} was 923 K, creep effects in terms of intergranular cracking became pronounced and rendered IP cycling more damaging in comparison to OP cycling.

2.3 Material for steam generator applications

2.3.1 Creep properties of modified 9Cr-1Mo Steel

Detailed investigation performed on the creep behaviour of indigenously developed steam generator (SG) tube steel and 70 mm forging in normalised and tempered condition at temperatures ranging from 823 to 923 K indicated that the creep-rupture strength of both SG tube steel and the forging are close to the strength values reported in the literature as well as specified in the French nuclear design code RCC-MR [27,28]. Figure 15 shows an example for above comparison at 823 K. The average and minimum creep-rupture strength values specified in RCC-MR for the steel at 823 K are also superimposed for comparison. However, 70 mm forging exhibited marginal lower creep-rupture strength compared to that obtained for SG tube steel. The analysis of creep data in terms of creep rate-rupture life relations indicated that the steel obeys Monkman-Grant and modified Monkman-Grant relationships. Further, a high creep damage tolerance factor obtained for the steel indicates resistance to localised cracking and this has been confirmed by the presence of transgraular fracture at the stress and temperature conditions examined. The tertiary creep was examined in terms of the variations of time to onset of tertiary creep with rupture life, and a recently proposed concept of time to attain Monkman-Grant ductility, and its relationship with rupture life that depends only on damage tolerance factor [28,29]. The extensive tertiary creep in modified 9Cr-1Mo steel appears to be generic to most of the 9%Cr ferritic steels and is ascribed to the effects associated with microstructural degradation such as coarsening of precipitates and dislocation substructure.

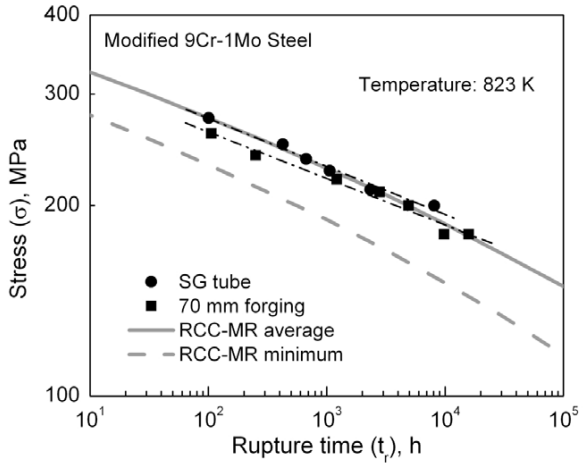

Fig. 15 : Stress vs. rupture time plots for indigenously developed SG tubes and 70 mm forging at 823 K. Average and minimum creep-rupture strength values specified in French nuclear design code RCC-MR for the steel at 823 K are also given for comparison.

2.3.2 Creep properties and Type IV cracking resistance of grade 91 weld joint

Fusion joining of modified 9Cr-1Mo steel results in a highly inhomogeneous microstructure across the joint [27]. A soft zone forms in the intercritical region of HAZ close to the unaffected base metal of the joint. The soft zone due to intercritical heating between AC_1 and AC_3 during weld thermal cycle results from the (i) replacement of martensite laths with high dislocation density in base metal by large sub-grains having low dislocation density, (ii) coarsening of $M_{23}C_6$ type of carbides at grain and sub-grain boundaries, and (iii) change in shape of the V/Nb carbonitride particles from needle to spherical and the reduction of their misfit with matrix. At relatively lower stresses and higher test temperatures, the weld joint possesses lower creep rupture life than the base metal, and the difference in creep rupture life increases with decrease in stress and increase in temperature (Fig. 16) [27]. Preferential accumulation of creep deformation coupled with extensive creep cavitation (Fig. 17) results in failure in the intercritical HAZ (Fig. 18), commonly known as type IV cracking. Micro-mechanistic effect of constraint deformation in the soft intercritical HAZ, which is sandwiched between highly inhomogeneous microconstituents of the joint, is considered as the reason for the premature failure. The constraint effects lead to the formation of micro-cracking and cavitation damage in the intercritical region of HAZ as shown in Fig. 19 for G91 steel

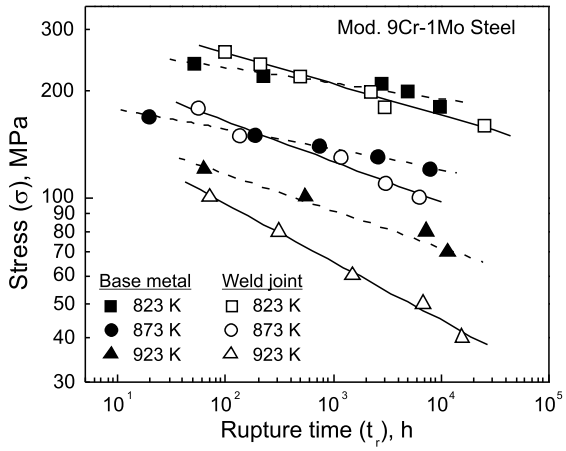

Fig. 16 : Stress vs. rupture life of base metal and weld joint of modified 9Cr-1Mo steel [30].

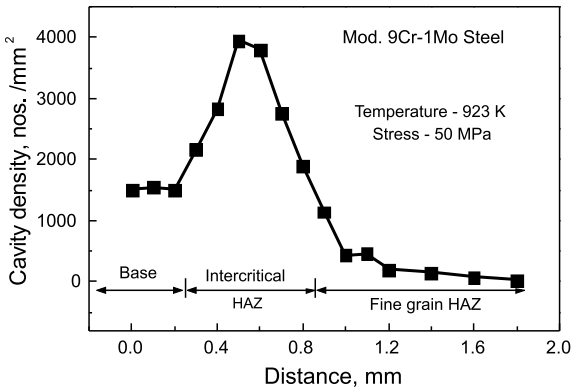

Fig. 17 : Distribution of creep cavities across weld joint in modified 9Cr-1Mo steel [30].

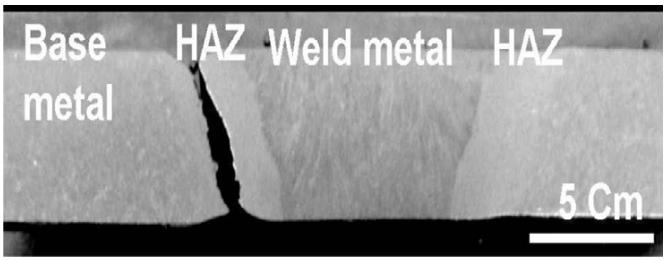

Fig. 18 : Typical type IV failure at the outer edge of HAZ in G91 weld joint specimen tested at 923 K and at 60 MPa for 1517 h [30].

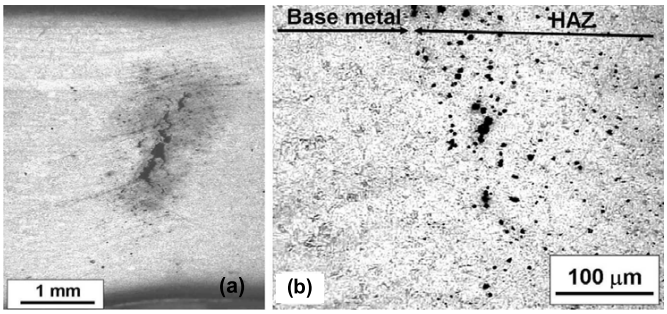

Fig. 19 : (a) Formation of macro-crack in HAZ in G91 steel weld joint tested at 823 K and at 160 MPa for 25422 h and (b) preferential creep cavitation in the intercritical region of HAZ in G91steel weld joint tested at 923 K and at 40 MPa for 15721 h [30].

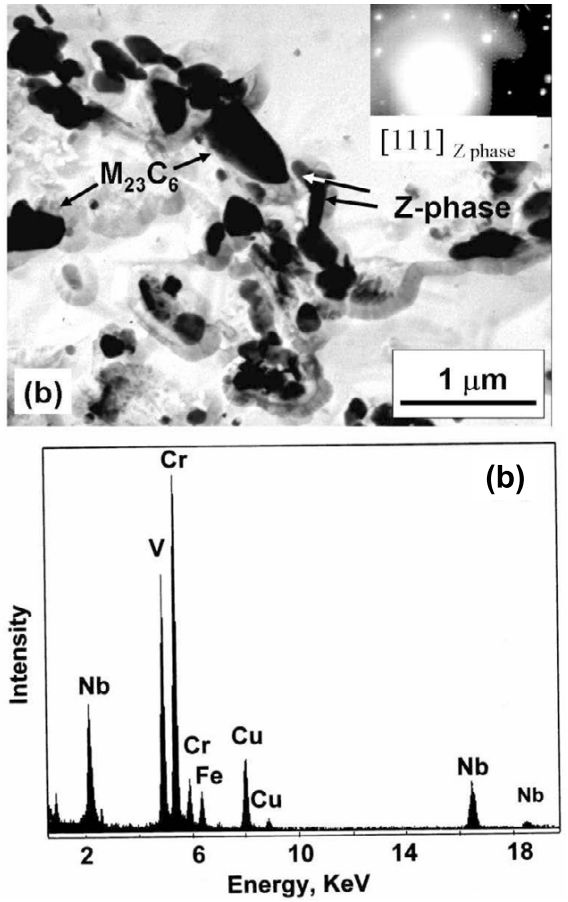

Fig. 20 : (a) TEM micrograph showing presence of Z-phase, a complex Cr(V,Nb)N particle in the intercritical HAZ of G91 weld joint tested for long duration. Energy dispersive X-ray spectrum of Z-phase is shown in (b).

weld joint. The type IV cracking susceptibility of modified 9Cr-1Mo steel is also enhanced with the precipitation of Z-phase, a complex Cr(V,Nb)N particle (Fig. 20) [30] in the intercritical HAZ of the joint. During long-term creep exposure, the Z-phase forms and grows rapidly at the expense of beneficial fine MX types of precipitates and accelerates the recovery in substructure with associated decrease in strength in the intercritical region of HAZ. Recent study [31] on advanced ferritic steels has shown that by controlled addition of boron and minimizing nitrogen content, resistance to Type IV cracking can be enhanced significantly. Microalloying with boron not only retards the coarsening of $M_{23}C_6$ by replacing some of its carbon but also significantly alter the microstructure of fine grain HAZ/coarse grain HAZ of the weld joint.

2.3.3 Low cycle fatigue properties of G91 steel

Low cycle fatigue behaviour of modified 9Cr-1Mo steel in different product forms namely rolled and forged plates and extruded pipe was investigated [32,33]. It was observed that both the rolled and extruded pipe of modified 9Cr-1Mo steel exhibit nearly similar stress response. The forged plate exhibited significantly lower stress response than those shown by rolled and extruded steels. Also, the forged steel displayed higher tensile ductility compared to that shown by rolled and extruded steels. The lower strength value of forged product was ascribed mainly to its coarse microstructure obtained during forging process. The plastic strain LCF resistance in terms of Coffin-Manson plots as shown in Fig. 21 was found to be higher for the forged steel compared to those exhibited by rolled and extruded products. The superior plastic strain LCF resistance of the forged steel can be attributed to higher ductility due to its coarse microstructure.

2.4 Creep and fatigue properties in flowing sodium

It is recognized that the synergistic effects of applied stress and flowing sodium are important for realistic evaluation of creep and fatigue properties of materials for sodium cooled fast reactor applications. The purity of sodium, material of construction of sodium loops, temperature and velocity of sodium and various other factors that determine mass transfer in the sodium circuit have a significant effect on creep and fatigue properties. In order to examine the

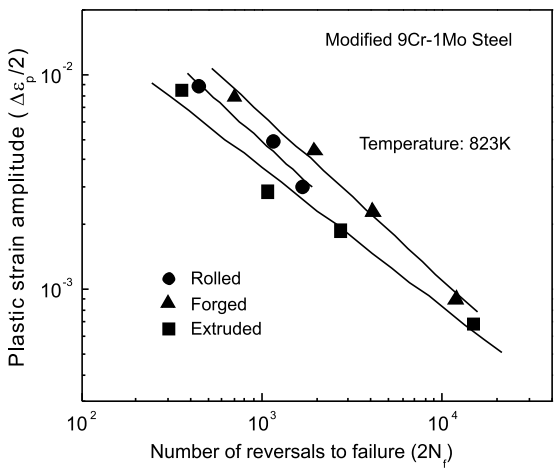

Fig. 21 : Coffin-Manson plots for modified 9Cr-1Mo steel for different product forms of rolled and forged plates and extruded pipe at 823 K.

effects of some of these variables on mechanical properties and to gain improved awareness for accurate life prediction, creep, low cycle fatigue and creep-fatigue tests in flowing sodium environment have been undertaken in in-sodium testing facility (INSOT) established at IGCAR. In the following, some of the recent results are described.

The stress vs. rupture time plots for 316L(N) stainless steel in air and in flowing sodium at 873 K as shown in Fig. 22 indicate improved rupture strength in sodium environment. The increase in rupture life is more pronounced at low stresses. LCF tests conducted in flowing sodium at 823 and 873 K have also shown that the LCF lives are significantly improved in sodium environment compared to that obtained in air environment. Fatigue lives in flowing sodium increased by a factor of 3 to 5.5 compared to the lives obtained in air environment. Figure 23 shows an example at 873 K. Lack of oxygen in sodium atmosphere plays a major role in enhancing fatigue life in sodium environment due to both the delayed crack initiation and reduced crack propagation. The delayed crack initiation and decreased crack growth rate result from absence of oxidation effects in a low oxygen atmosphere in flowing sodium.

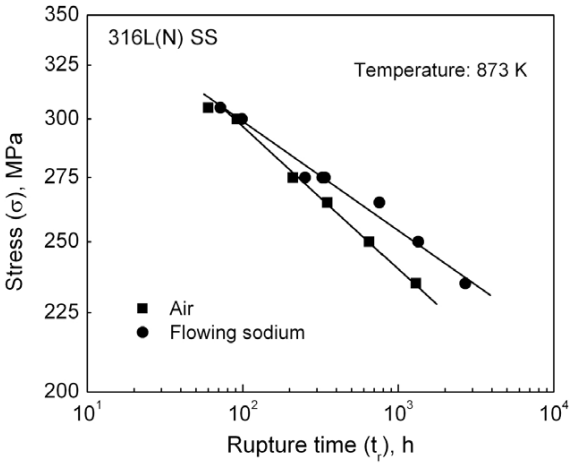

Fig. 22 : Stress vs. rupture life plots for 316L(N) SS in air and flowing sodium environments at 873 K.

3. Future directions

There would be considerable benefits in developing new structural materials, where high operating temperatures and strength coupled with resistance to neutron induced void swelling and irradiation embrittlement are major considerations. In order to extend the life of fuel cladding for achieving high burnup, materials that exhibit superior resistance to high neutron exposure beyond 200 dpa as well as high creep strength at 973 K are needed. ODS ferritic/ martensitic steels, which have higher swelling resistance and creep strength than Alloy D9 or D9I are currently under development. The ODS alloys derive their strength from dispersions of nano-sized clusters of oxygen atoms stabilised by elements such as Y and Ti [9]. Excellent progress has been achieved in improving resistance to creep by control of nanocluster composition, number density and stability. The fine dispersion of yttria (Y_2O_3) improves high temperature strength by hindering mobile dislocations and also retards irradiation swelling by acting as trapping sites for point defects induced by irradiation. The addition of a small amount of titanium further reduces the size of oxide particles to 2-3 nm and hence inter-particle spacing that significantly improves creep rupture strength. Currently, 9Cr-ODS steel

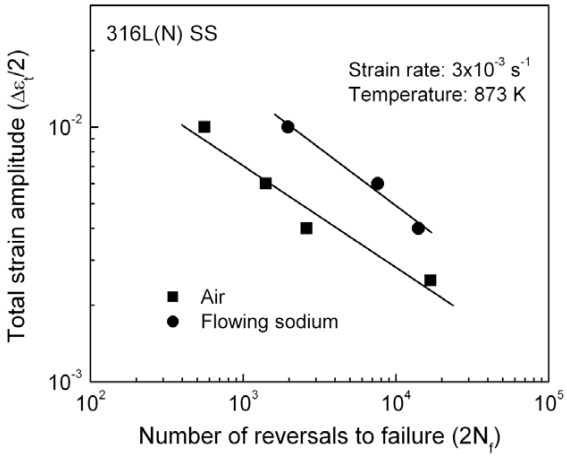

Fig. 23 : Comparison of LCF lives of 316L(N) SS in air and sodium environments at 873 K.

with composition of 9Cr-0.12C-2W-0.2Ti-0.37Y_2O_3 has received international consideration. Low fracture toughness, high ductile-to-brittle transition temperature (DBTT) [10] and finding suitable welding process (fusion welding is undesirable) for ODS alloys continue to be the causes of concern. Much more work is needed on ODS steels before they can be used in critical structural components such as SFR cladding.

Austenitic steels used for wrapper application suffer from bowing of subassemblies due to differential void swelling and this result in severe handling problems thereby restricting the fuel burnup. In order to overcome this problem, 9%Cr ferritic steel has been chosen as an alternate and is being developed for future wrapper applications [6-8]. It is known that 9% Cr steel displays reasonable high creep strength to satisfy the creep strength requirements for wrapper application. The only issue with ferritic steels is that they undergo ductile-brittle transition. By modifying the chemistry and lowering the trace elements such as sulphur and phosphorous as well as by choosing clean steel making route, it has been possible to develop the steel with ductile-brittle transition temperature much lower than room temperature. Further work is in progress to optimise composition and grain size following examination of critical issues such as irradiation as well as thermal ageing effects.

For out-of-core structural components in PFBR, a reduced carbon and controlled nitrogen added 316L(N) SS is being used. In order to increase the design life of structural components in future SFRs to 60 years, work towards optimisation of increased nitrogen content for further improvement in long-term creep and creep-fatigue properties of 316LN SS has been undertaken. Efforts are being made to assess long-term microstructural stability for long-term creep and creep-fatigue strengths for reliable extrapolation to the enhanced design life. Appropriate analytical techniques involving microstructural details and their modifications for reliable prediction of creep and creep-fatigue lives for design life of 60 years are being examined. Attempts are being made to increase type IV cracking resistance of G91 weld joints critical for SG application through selection of suitable heat treatment for the reduction/elimination of strength inhomogeneity across the weld joint, increase in the width of HAZ for reduced stress triaxiality resulting in lower constraint for deformation of soft intercritical region and thereby creep cavitation, addition of solid solution strengthening elements like W, Re and Co for increased resistance to softening of intercritical HAZ and by micro alloying with boron.

4. Concluding remarks

The important role of SFRs to deliver considerable percentage of future electricity generation in the country has been highlighted. The importance of materials and the required relevant properties like resistance to radiation damage and high temperature mechanical properties particularly creep and fatigue issues for reactor core, out-of-core and steam generator applications in developing robust, safe and economical SFR technology are described. The recent results and important outcome from in-house science based research and development towards achieving high creep and fatigue resistant materials for SFR applications are presented. Special emphasis has been placed in developing indigenous materials with improved creep and fatigue properties for different components for fast reactor applications. Unique and improved material properties obtained for core material such as creep properties of Alloy D9 with different Ti/C ratio, and creep, low cycle fatigue and thermo-mechanical fatigue behaviour of base, weld and weld joints of 316L(N) SS along with material behaviour in flowing sodium environment for structural applications are demonstrated. Creep and fatigue behaviour of G91 steel along with type IV cracking resistance of weld joints important for steam generator applications are presented. In order to achieve high fuel burnup for economical nuclear energy, a roadmap highlighting the relevant science and technological goals has been drawn up for the development of advanced materials for clads such as improved D9I and ODS alloys and wrappers made of 9% Cr steels, and enhanced design life of sixty years for out-of-core structural components.

Acknowledgements

The authors thank Dr. T. Jayakumar, Director, Metallurgy and Materials Group and Dr. M. D. Mathew, Head, Mechanical Metallurgy Division for stimulating discussions during the preparation of the manuscript. The valuable contributions from the scientists and engineers of Metallurgy and Materials Group are gratefully acknowledged.

References

1. Baldev Raj, in *Pressure Vessels and Piping: Codes, Standards, Design and Analysis*, Eds. Baldev Raj, Choudhary B K and Velusamy K, Narosa Publishing House, New Delhi, (2009) 1.
2. Mannan S L, Chetal S C, Baldev Raj and Bhoje S B, *Trans. Indian Inst. Met.,* **56** (2003) 155.
3. Seran J L, Levy V, Dubuisson P, Gilbon D, Maillard A, Fissolo A, Touron H, Cauvin R, Chalony A and E Le Boulbin, in *Effects of Radiation Materials:15th International Symposium ASTM STP 1125*, eds. Stoller R E, Kumar A S and Gelles D S, American Society for Testing and Materials, Philadelphia, (1992) 1209.
4. Herschbach K, Schneider W and Ehrlich K, *J. Nucl. Mater.,* **203** (1993) 233.
5. Mannan S L and P. V. Sivaprasad, in *Encyclopedia of Materials Science and Engineering,* eds. K. H. Jurgen Buschow, Robert W. Cahn, Merton C. Flemings, Bernhard Ilschner, Edward J. Kramer and Subash Mahajan, Elsevier, New York, **3** (2001), 2857.
6. Dubuisson P, Gilbon D and Seran J L, *J. Nucl. Mater.,* **205** (1993) 178.
7. High Chromium Ferritic and Martensitic Steels for Nuclear Applications, eds. Klueh R L and Harries D R, *American Society for Testing and Materials, Pa,* (2001) 90.
8. Kohyama A, Hishinuma A, Gelles D S, Klueh R L, Dietz W and Elrich K, *J. Nucl. Mater.,* **233-237** (1996) 138.
9. Ukai S, Mizuta S, Fujiwara M, Okuda T and Kobayashi T, *J. Nucl. Sci. Technol.,* **39** (2002) 778.
10. R. Lindau A. Möslang, Rieth M, Klimiankou M, Materna-Morris E, Alamo A, A.-A. F. Tavassoli, Cayron C, A.-M. Lancha, Fernandez P, Baluc N, Schäublin R, Diegele E, Filacchioni G, Rensman J W, B.v.d. Schaaf, Lucon E and Dietz W, *Fusion Eng. Des*., **75** (2005) 989.
11. Choudhary B K, Phaniraj C, Rao K B S and Mannan S L, *Key Eng. Mater.,* **171-174** (2000) 437.
12. Choudhary B K, Phaniraj C, Rao K B S and Mannan S L, *ISIJ Inter*. Supplement. **41** (2001) S73.
13. Phaniraj C, Choudhary B K, Rao K B S, and Baldev Raj, *Scripta Materialia,* **48** (2003) 1313.
14. Phaniraj C, Choudhary B K, Baldev Raj and Rao K B S, *J. Mater. Sci.*, **40** (2005) 2561.
15. Phaniraj C, Choudhary B K, Baldev Raj and Jayakumar T, *Mater. Sci. Eng. A*, **398** (2005) 373.
16. Phaniraj C, Choudhary B K and Baldev Raj, in *Pressure Vessels and Piping: Materials and Properties*, Eds. Baldev Raj, Choudhary B K and Anish Kumar, Narosa Publishing House, New Delhi, (2009) 183.
17. Latha S, Mathew M D, Rao K B S and Mannan S L, *Trans. Indian Inst. Met*., **49** (1996) 587.
18. Latha S, Mathew M D, Rao K B S and Mannan S L, *Trans. Indian Inst. Met*., **58** (2005) 343.
19. Divakar R, Banerjee A, Raju S and Mohandas E, Proc. Conf. *Physical Metallurgy Research, Techniques and Applications*, Mumbai, India, December 2004.
20. Mathew M D, Sasikala G, Rao K B S and Mannan S L, *Mater Sci Engg. A*, **148** (1991) 253
21. Girish Shastry, Mathew M D, Rao K B S and Mannan S L, *Trans. Indian Inst. Met*., **58** (2005) 275.
22. Sasikala G, Mathew M D, Rao K B S and Mannan S L, *Metall. Mater. Trans. A*, **31** (2000) 1175.
23. Ganesan V, Mathew M D, Rao K B S and Baldev Raj, in Proc. 6th European stainless steel conference - science and market, Helsinki, 2008, eds. Pentti Karjalainen and Staffan Hertzman, (2008) 445.
24. Srinivasan V S, Valsan M, Sandhya R, Rao K B S, Mannan S L and Sastry D H, *Int. J. Fatigue*, **13** (1991) 471.
25. Srinivasan V S, Valsan M, Rao K B S, Mannan S L and Baldev Raj, *Int. J. Fatigue*, **25** (2003) 1327.
26. Nagesha A, Valsan M, Kannan R, Rao K B S, Bauer V, Chris H J and Vakil Singh, *Int. J. Fatigue,* **31** (2009) 636.
27. Choudhary B K, Laha K, Nagesha A, Isaac Samuel E, Srinivasan V S, Chandravati K S, Valsan M, Kannan R, Rao K B S and Mannan S L, in Proc. Seminar on *Materials R & D for PFBR*, Kalpakkam, India, (2003) 121.
28. Isaac Samuel E, Choudhary B K, Rao K B S and Mannan S L, *Trans. Indian Inst. Met*., **58** (2005) 287.
29. Isaac Samuel E, Choudhary B K, Rao K B S and Baldev Raj, in *Pressure Vessels and Piping: Materials and Properties*, Eds. Baldev Raj, Choudhary B K and Anish Kumar, Narosa Publishing House, New Delhi, (2009) 83.
30. Laha K, Chandravathi K S, Parameswaran P, Rao K B S and Mannan S L, *Metall. Mater. Trans. A*, **38** (2007) 58.
31. Albert S K, Kondo M, Tabuchi M, Yin F, Sawada K and Abe F, *Metall. Mater. Trans. A*, **36** (2005) 333.
32. Nagesha A, Valsan M, Kannan R, Rao K B S, Mannan S L, *Int. J. Fatigue*, 24 (2002) 1285.
33. Vani Shankar, Valsan M, Rao K B S, Kannan R, Mannan S L and Pathak S D, *Mater. Sci. Engg. A*, **437** (2006) 413.